CHEMISTRY
A EUROPEAN JOURNAL

DOI: 10.1002/chem.200801055

Electronic and Vibronic Contributions to Two-Photon Absorption in Donor–Acceptor–Donor Squaraine Chromophores

Shino Ohira, Indranil Rudra, Karin Schmidt, Stephen Barlow, Sung-Jae Chung, Qing Zhang, Jon Matichak, Seth R. Marder, and Jean-Luc Brédas*[a]

Abstract: Many squaraines have been observed to exhibit two-photon absorption at transition energies close to those of the lowest energy one-photon electronic transitions. Here, the electronic and vibronic contributions to these low-energy two-photon absorptions are elucidated by performing correlated quantum-chemical calculations on model chromophores that differ in their terminal donor groups (diarylaminothienyl, indolenylidenemethyl, dimethylaminopolyenyl, or 4-(dimethylamino)phenylpolyenyl). For squaraines with diarylaminothienyl and dimethylaminopolyenyl donors and for the longer examples of 4-(dimethylamino)-phenylpolyenyl donors, the calculated energies of the lowest two-photon active states approach those of the lowest energy one-photon active ($1B_u$) states. This is consistent with the existence of purely electronic channels for low-energy two-photon absorption (TPA) in these types of chromophores. On the other hand, for all squaraines containing indolinylidenemethyl donors, the calculations indicate that there are no low-lying electronic states of appropriate symmetry for TPA. Actually, we find that the lowest energy TPA transitions can be explained through coupling of the one-photon absorption (OPA) active $1B_u$ state with b_u vibrational modes. Through implementation of Herzberg–Teller theory, we are able to identify the vibrational modes responsible for the low-energy TPA peak and to reproduce, at least qualitatively, the experimental TPA spectra of several squaraines of this type.

Keywords: chromophores · nonlinear optics · squaraines · two-photon absorption · vibronic coupling

Introduction

Organic materials with large two-photon absorption (TPA) cross sections (δ) are of interest due to potential optical, materials fabrication, and biological applications.[1–6] High TPA cross sections have been observed for chromophores with various structural motifs, including donor–acceptor–donor (D-A-D) conjugated chromophores. Among this class of chromophores, the linear and nonlinear optical properties of D-A-D squaraines (also known as squarylium dyes) consisting of two electron-donor terminal groups (D) and a central electron-poor 1,3-disubstituted C_4O_2-unit (A) have been extensively studied, because of their narrow and intense one-photon absorption (OPA) bands and large real and imaginary third-order non-linear optical (NLO) responses.[7–22]

High TPA cross sections ranging from 750[13] to 33 000 GM[16] (1 GM [Goeppert-Mayer] $= 10^{-50}$ cm^4 s^{-1} per photon) have been measured at photon energies close to the OPA edge for a variety of squaraines. Assuming centrosymmetric conformations,[1] this corresponds to excitation to a

[a] S. Ohira, Dr. I. Rudra, Dr. K. Schmidt, Dr. S. Barlow, Dr. S.-J. Chung, Dr. Q. Zhang, J. Matichak, Prof. S. R. Marder, Prof. J.-L. Brédas
School of Chemistry and Biochemistry and
Center of Organic Photonics and Electronics
Georgia Institute of Technology, Atlanta
Georgia 30332–0400 (USA)
Fax: (+1) 404-894-7452
E-mail: jean-luc.bredas@chemistry.gatech.edu

Supporting information for this article is available on the WWW under http://dx.doi.org/10.1002/chem.200801055. It contains the complete synthetic procedures and characterization data for the new squaraine compounds **2**, **7**, and **8**, the details of the TPA measurements, and the details of the quantum-chemical calculations

[1] Even though, as discussed in the results and discussion section, squaraine compounds can adopt several non-centrosymmetric conformations, the behavior of their excited states typically remains strongly reminiscent of the properties of strictly *ungerade* and *gerade* states found in the centrosymmetric conformers; this is particularly true for extended molecules. We have, therefore, referred to all excited states assuming inversion symmetry, that is, as (one-photon active) B_u or (two-photon active) A_g states, even if the structure of a particular conformer deviates from centrosymmetry.

singlet A_g state referred to here as peak 3 (see Figure 1 for general peak labeling). Some of these cross sections are remarkably large, even when normalized for the number of π

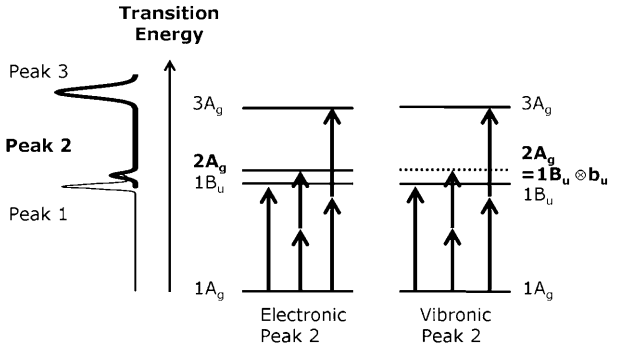

Figure 1. Illustration of the one-photon (light line) and two-photon (bold line) absorption processes in squaraines. Left: Sketch of the absorption spectra of squaraines. Middle: peak 2 is purely electronic. Right: peak 2 has the same electronic nature as the $1B_u$ state.

electrons in the molecules, and originate largely from resonance enhancement, that is, from the appropriate photon energy closely approaching the one-photon transition energy.[16] It is worth pointing out that is possible to observe the effects of resonance enhancement, that is, to probe TPA with excitation energies very close to the OPA transition, due to the remarkably sharp OPA absorption edge. However, in squaraines with indolinylidenemethyl donor groups, in addition to the strong high-energy TPA state, there is evidence for another TPA state (referred to here as peak 2) at state energy similar to that of the lowest energy OPA transition; this lower energy TPA then occurs with maxima in the near-infrared spectral region at photon wavelengths of 1.1–1.4 μm, with cross sections ranging from 45[15] to 500 GM[13] (this is shown below for the new compound **8** in Figure 2). Recently, we have also found a low-energy TPA active state

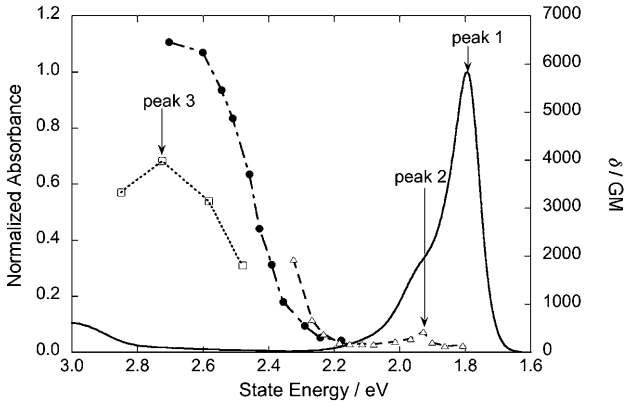

Figure 2. OPA spectrum of **8** (solid line) compared with a degenerate TPA spectrum from Z-scan measurements (open squares, dotted line) and with nondegenerate TPA spectra acquired using the WLC method with pump wavelengths of 1180 and 1600 nm (solid circles, dot-dash line and open triangles, dashed line, respectively). All data were acquired in CH_2Cl_2 solution.

at energy similar to the lowest OPA active state in an example of a squaraine in which the donors are substituted pyrroles with extended conjugation, with cross sections of 800 and 1600 GM at photon wavelengths of 1.3 and 1.5 μm, respectively.[16] Despite the cross section of peak 2 typically being considerably lower than that of the near-resonant state (peak 3), peak 2 can be of importance for optoelectronic applications, since, depending on the molecular structure, this absorption is located close to or within the telecommunications band of the near-infrared (1.30–1.55 μm). TPA in this region can potentially be exploited for applications such as all-optical beam stabilization and dynamic range compression, while the presence of a TPA-allowed state close to this region will affect the telecommunication-band dispersion of the real part of the third-order polarizability γ, which can be exploited for all-optical switching.

To take full advantage of such TPA in the near-IR region, it is important to better understand the origin of the associated excited state. However, previous quantum-chemical studies on such compounds have considered only purely electronic channels for TPA and have neither addressed the nature of this state in detail nor been successful in reproducing the small energetic separations observed between peak 1 (the OPA peak) and peak 2, that is, in general < 0.2 eV.[17–20] Rather than assigning peak 2 to a low-lying electronic state, Scherer et al. proposed an alternative origin for peak 2,[13] suggesting the possibility of vibronic coupling between the first excited electronic $1B_u$ state and vibrational modes of b_u symmetry. Furthermore, the presence of both centroymmetric and non-centrosymmetric conformational isomers, which is supported by NMR experiments for certain squaraines,[21,23] has also been put forward as an explanation for the closely spaced peaks 1 and 2;[20,21] in this case, peak 2 would primarily originate from the lowest electronic excited state, that is, a strongly OPA active state, of the non-centrosymmetric conformers. In such non-centrosymmetric conformers, the OPA active state is not of strict *ungerade* (i.e., B_u) character and can, therefore, in principle, exhibit a non-zero TPA cross section due to TPA through purely electronic channels. The observed energetic offset between the OPA peak 1 and TPA peak 2 signals could then potentially be attributed to somewhat different OPA state energies for centrosymmetric and non-centrosymmetric conformers.[2]

Thus, there can be three possible origins for the lowest-energy TPA active state in squaraines: 1) peak 2 is primarily of electronic nature and due to TPA into the lowest OPA excited states of noncentrosymmetric conformers; 2) peak 2 is primarily electronic in nature and arises from a TPA-allowed $2A_g$ state close in energy to the OPA-allowed $1B_u$; or 3) the state corresponding to peak 2 has the same electronic nature as the OPA $1B_u$ state, but acquires cross section due to vibronic coupling (non-zero coupling of $1B_u$ state to higher lying A_g states (Figure 1) through b_u modes). In the

[2] Moreover, the TPA maximum is typically shifted towards higher energies with respect to the corresponding OPA maximum, since Franck–Condon coupling can redistribute TPA cross section from the (0–0) into the (0–1) vibrational transition.[22]

third scenario, the electronic sum-over-states model must be extended to account for vibronic coupling. In the linear coupling regime, this can be achieved by applying Herzberg–Teller (HT) theory.[24]

In this contribution based on joint theoretical and experimental studies, we seek to provide insight into various structural aspects of squaraines that can lead to a peak 2 absorption in their TPA spectra through one of the three different origins described in the previous paragraph or a combination thereof. Here, we consider a series of squaraines with different terminal donor groups. To ease the systematic study of their TPA spectra, the squaraines we have experimentally studied have been classified into different groups depending on the nature of their terminal groups:

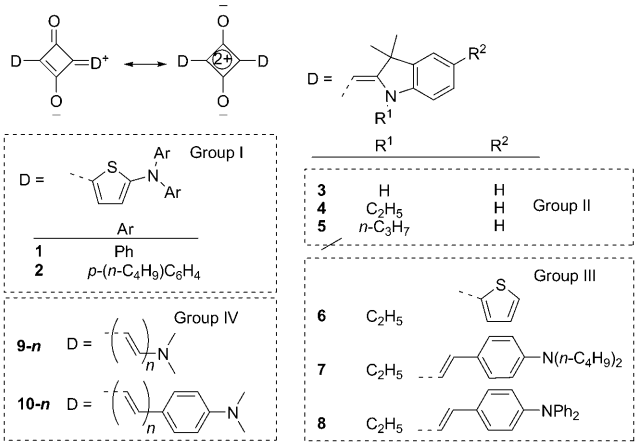

1) Group I consists of squaraines with diarylaminothienyl donors, new compound **2** and model compound **1**.
2) Group II consists of squaraines **3–5** (**4** being used as a model for **5**), in which the *N*-alkylation of indolinylidenemethyl donors is varied.
3) Group III consists of **6** and new compounds **7–8**, in which the role of attaching additional π-conjugated groups to the 5-position of indolinylidenemethyl donors is investigated.
4) On the theoretical side, we also consider the hypothetical compounds of group IV, in which the effect of increasing the π-conjugation length ($n=1$–4) between the terminal donor and central acceptor units are studied in the model dimethylaminopolyenyl and 4-(dimethylamino)-phenylpolyenyl-substituted squaraine series **9-*n*** and **10-*n***.

The TPA spectra of compounds **2**, **7**, and **8** are reported for the first time, while TPA spectra for **3–6** can be found in the literature.[13,15,18]

This paper is structured as follows. First, we describe the TPA spectra available for the compounds investigated here. We then discuss the results of computational studies on the effect of molecular conformation on the TPA spectra, focusing on the possibility of TPA into the lowest lying OPA state of non-centrosymmetric conformers. We turn next to a theoretical analysis of the possibility of low-lying electronically allowed TPA states in the different types of squaraines under consideration. Finally, we investigate how vibronic coupling of the lowest OPA state to antisymmetric vibrational modes can give rise to low-energy TPA in squaraines with indolinylidenemethyl donors.

Results and Discussion

Two-photon spectra: The TPA spectra for **4**, **5**, and **6** have previously been acquired by using Z-scan and two-photon-induced fluorescence methods,[13,15] while the positions of peaks 2 and 3 in the TPA spectrum of **3** have been obtained from the spectral dispersion of third-harmonic generation.[18] The three group II squaraines, **3–5**, are all reported to show OPA (peak 1) at a state energy of 1.95 eV, a low-energy TPA peak (peak 2) at approximately 2.1 eV, and a strong TPA peak (peak 3) at higher energy (3.0 eV for **4** and **5** and 3.3 eV in the case of **3**, for which the maximum is only imprecisely determined).[3] The previously studied type-III squaraine **6** shows OPA and TPA spectra qualitatively similar to the group II examples, but with all excited states observed at slightly lower energy. The new compounds **2**, **7**, and **8** were synthesized as described in the Supporting Information; degenerate and non-degenerate two-photon spectra were acquired by the group of Prof. E. W. Stryland at the University of Central Florida using the open-aperture fs Z-scan technique[25,26] and the white-light continuum (WLC) pump-probe method.[27] The TPA spectra for compound **8** are shown in Figure 2, while those for **2** and **7** are given in the Supporting Information (S2-1 and S2-2). As shown in Figure 2, the WLC data afford larger cross sections than the Z-scan data; these cross sections increase as the wavelength difference between pump and probe is increased, as expected from pre-resonance enhancement effects.[28] Compound **2** shows no clear maximum in the high-energy TPA feature (peak 3); however, the data suggest a degenerate TPA peak cross section of at least 1300 GM at a detuning energy of less than 0.25 eV (the detuning energy corresponds to the difference between the OPA energy and the fundamental photon energy). Compounds **7** and **8** show high-energy TPA maxima (peak 3) with degenerate cross sections of 3000–4000 GM at detuning energies of about 0.4–0.5 eV. All three compounds show low-energy TPA peaks (peak 2) with maxima at state energies some 0.13–0.14 eV higher in energy than the OPA maxima (peak 1) with non-degenerate TPA cross sections of a few hundred GM (degenerate TPA cross sections would be anticipated to be somewhat smaller). The OPA and TPA spectra for **7** and **8** closely resemble those for the other group III squaraine previously reported by Scherer et al., compound **6**, in terms of detuning energies and TPA cross sections, the main difference being that the

[3] An additional high-energy TPA peak was observed for **4** at about 3.5 eV.[15] In another example of a group II squaraine ($R^1=Me$, $R^2=H$) only the high-energy range was studied; however, peak 1 and 3 energies were similar to those reported for **4** and **5**.[22]

excited-state energies are consistently about 0.1 eV lower in the present compounds.

Effect of coexistence of different conformers: We first studied the effect of molecular (centrosymmetric and non-centrosymmetric) conformations on the TPA spectra of squaraines, in order to investigate the likelihood that the experimentally observed lowest lying two-photon active peaks, that is, peak 2, could be attributed to purely electronic TPA into the lowest lying one-photon state of non-centrosymmetric conformers. Among the investigated squaraines, we found that, in general, the approximately planar C_{2h}/C_i centrosymmetric (conformers **i** and **iii**) and the C_{2v}/C_2 non-centrosymmetric conformers (conformers **ii** and **iv**) are more stable relative to conformations with a twisted π-systems[4] and are, thus, likely to predominate at room temperature. Among squaraines **1** (used as a model for experimentally studied compound **2**), **3** and **4**, it is only in the case of **3** that the non-centrosymmetric conformation (**3″**; conformation **ii**) is energetically more favorable than the centrosymmetric conformer (**3′**; conformation **i**); the energy difference between the **3′** and **3″** isomers calculated at the B3LYP/SV(P) level is 0.06 eV (equivalent to ≈700 K). These results are in agreement with those of the theoretical and experimental work of Dirk et al.,[21] in which the larger stability of **3″** compared to **3′** had been attributed to the formation of energetically more stable hydrogen bonds in **3″** between both of the indole-ring nitrogen atoms and the same carbonyl oxygen atom of the central unit.

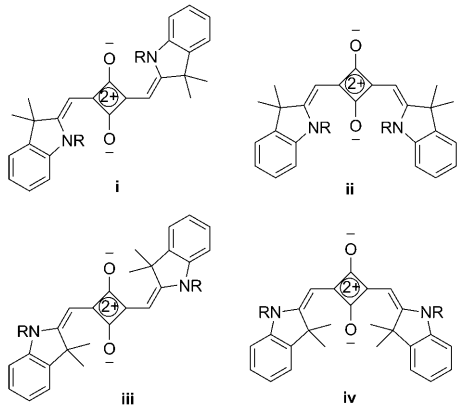

In the case of squaraines **4′** (centrosymmetric) and **4″** (non-centrosymmetric), the possibility for strong hydrogen bonding is removed, while steric hindrance effects between donor and acceptor groups increase as the hydrogen atoms are replaced by alkyl groups. As a result, **4′** is more stable than **4″** by 0.22 eV (equivalent to ≈2,500 K). On the other hand, the energy difference between the two isomers of squaraine **1** was computed to be negligibly small. Although our calculations indicate that the non-centrosymmetric conformation **iv** and centrosymmetric conformation **iii** have slightly higher energies compared to conformations **ii** and **i** for squaraines **3** and **4**, respectively, the possibility of isomeric mixtures (**i** and **iii** or **ii** and **iv**) cannot be completely ruled out in solution at ambient temperature. Thus, assuming that solvation does not substantially affect the relative energies of the conformers, squaraines **1**, **3**, and **4** are predicted to be present at ambient temperature as a mixture; that is, **3** predominantly as the C_{2v}/C_2 conformer (mostly **ii** and probably **iv**), **4** overwhelmingly as the C_{2h}/C_i conformer (mostly **i** and probably **iii**), and **1** as a mixture in which no particular conformer is dominant. We now discuss the electronic structures and TPA activity for these two conformers in squaraines **1**, **3**, and **4**.

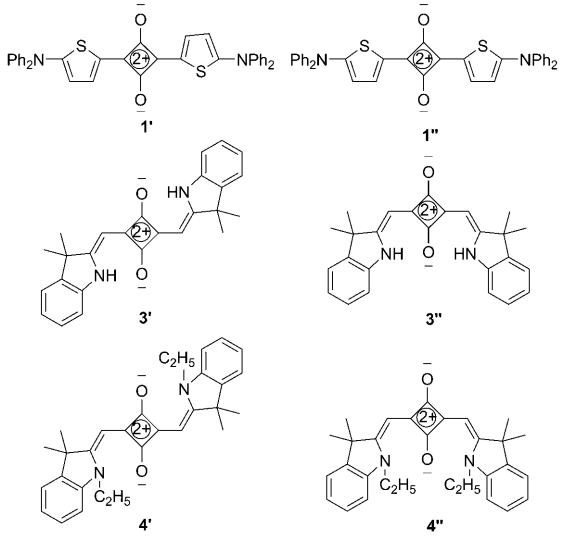

INDO/MRDCIS calculations (see Tables S3-2, S3-9 and S3-11 in Supporting Information for details) suggest very similar OPA and TPA spectra for both centro- and non-centrosymmetric conformers of **1**, **3**, and **4**. This is true irrespective of which isomers (**i–iv**) are considered (we present the theoretical details for squaraine **4** in table S3–19 under Supporting Information). In particular, the TPA cross section of the lowest OPA active state, S_1, remains negligibly small (<4 GM); therefore, purely electronic TPA channels into S_1 in the non-centrosymmetric conformers can be ruled out as a possible origin of peak 2. By taking squaraine conformers **3′** and **3″** as representative examples, we can distinguish two reasons for this absence of TPA-activity for the lowest OPA state, despite the lack of an inversion center. Since **3″** has a non-zero static dipole moment, change of this dipole moment upon excitation to the one-photon state could, in principle, give rise to a non-zero TPA cross section. How-

[4] Roughly planar geometries were observed in NMR experiments by Dirk et al.[21] as well as in crystal structures obtained by Kobayashi et al.[29] In the case of conformation **i** of squaraine **3**, semiempirical INDO/MRDCI calculations on the isolated molecule indicate that the conformation with a twist of 10° is 0.12 eV higher in energy than the fully planar conformation, suggesting the existence of mostly planar structures.

ever, the excited state in both squaraine conformers **3′** and **3″** can be described principally as arising from a HOMO–LUMO transition. The HOMO and LUMO of the molecule (Figure 3) indicate rather little change in the spatial extent

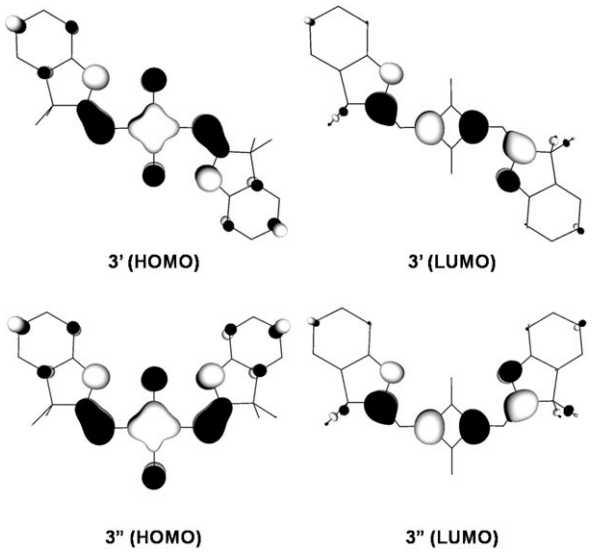

Figure 3. Representation of the HOMO (highest occupied molecular orbital) and LUMO (lowest unoccupied molecular orbital) wavefunctions for two conformations of **3**, calculated at the DFT-B3LYP/SV(P) level.

of the electron-density distribution and, as a result, the change in static dipole moment between the two states ($\Delta\mu_{01}$) is also quite small ($\approx$0.1 D), while the corresponding transition dipole moment (M_{01}) is large ($\approx$10 D). Considering the relation between $\Delta\mu_{01}$, M_{01} and TPA cross section δ according to the two-state model for TPA into the $1B_u$ state,[10,30–32] $\delta \propto (\Delta\mu_{01}^2 M_{01}^2)/(E_{01}-\hbar\omega)^2$ (in which $\hbar\omega$ is the fundamental photon energy), it can be easily understood why a small $\Delta\mu_{01}$ would result in a very small TPA cross section for the first excited state of squaraine **3″**.

Possible electronic origin of lowest TPA state (peak 2): In the previous section, we demonstrated that non-centrosymmetric conformers do not exhibit significant TPA cross sections into S_1, the lowest energy OPA state, through purely electronic channels. Considering the close similarity of the OPA and TPA spectra calculated for centro- and non-centrosymmetric conformers, we will henceforth restrict our discussion to the centrosymmetric conformers.[5]

To find out whether structural modifications of the terminal donor group can result in a TPA active electronic state at the position of peak 2, we now turn to a systematic study of the OPA and TPA spectra of squaraines belonging to groups I, II, III, and IV. As in the previous section, we use squaraine **1** to model new compound **2**. The INDO/MRDCI computed energies of the lowest OPA and TPA active states of **1** are 1.76 and 2.02 eV, respectively, which are in good agreement with the experimental peak 1 and peak 2 maxima of 1.77 and 1.92 eV, respectively, found for **2** (Figure 4). A second TPA peak between 2.8 and 3.7 eV[6] is consistent with the experimental feature at higher energy, which apparently represents the tail of a TPA feature with a maximum at a state energy of approximately 3 eV or higher. It is interesting to note that the lowest TPA active state is quite close in energy (calculated to be within 0.26 eV) to the OPA active $1B_u$ state. We would like to point out that a similar energy-level alignment of peak 2 (with TPA cross section less than 100 GM) with respect to peaks 1 and 3 was calculated for some extended pyrrole-substituted squaraines[16] (see the Supporting Information of reference [16], section on Details of Quantum Chemical Calculations). The similar behavior of the compounds discussed in reference [16] to that of **1** and **2**, in contrast to that for group II and III squaraines (vide infra), thus suggests that they can also be classified as group I compounds. Note that, although the calculations suggest that peak 2 for this group is principally electronic in origin, some contributions from vibronic coupling cannot be ruled out. The model squaraines of group IV also exhibit low-energy TPA active states (see Figure 5). In general, the lowest TPA state falls in energy with conjugation length more rapidly than the OPA state.

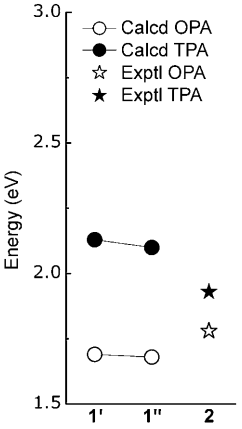

Figure 4. INDO/MRDCIS-calculated state energies for two conformers of **1**. See Supporting Information for the experimental spectra of **2**.

In contrast to groups I and IV, a TPA active electronic state was not calculated to appear in the vicinity of experimental peak 2 (i.e., close to peak 1) in the bis(indolinylidenemethyl) species of groups II and III. Instead, the calculated OPA state energies and the lowest electronic TPA active state energies of the molecules were consistent with the experimental values for peaks 1 and 3, with two TPA states appearing in the vicinity of the experimentally observed peak 3 (Figure 6). The energies of both transitions are rather insensitive to alkylation on the indole nitrogen atoms (**4** vs. **3**) and also to extension of conjugation at the 4-position of the indole ring system in series III. The insensitivity to extended conjugation reflects the lack of a direct conjugation pathway from the six-membered ring of the indole to the squarylium acceptor; this can be seen from the localiza-

[5] In the context of having multiple species (such as conformers) possibly simultaneously present, it is worth noting that the existence of broken-symmetry structures (in either ground or first excited states), analogous to those seen in a few cyanines, can be ruled out due to the absence of substantial solvatochromism in absorption or fluorescence spectra.[22]

[6] Exact assignment of the TPA peak is made ambiguous due to the presence of multiple calculated TPA active electronic states in the higher energy region of interest (see Tables S3–16, S3–17, and S3–18 in Supporting Information for details).

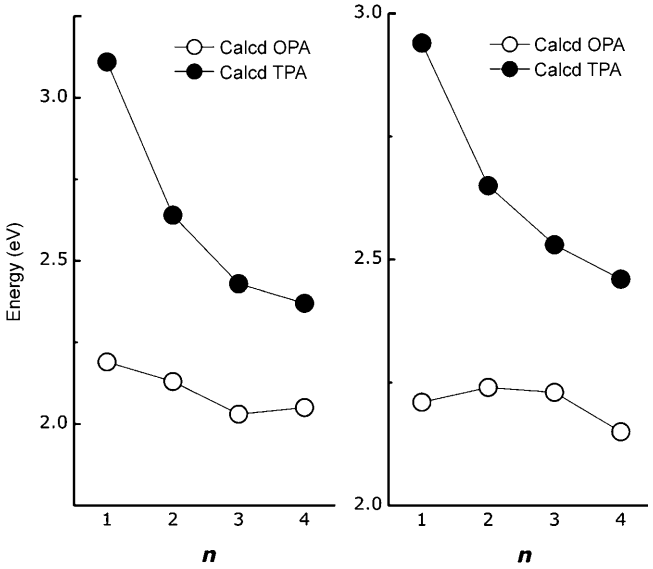

Figure 5. INDO/MRDCIS-calculated state energies of **9** (left) and **10** (right) as a function of size of the polyenic segment.

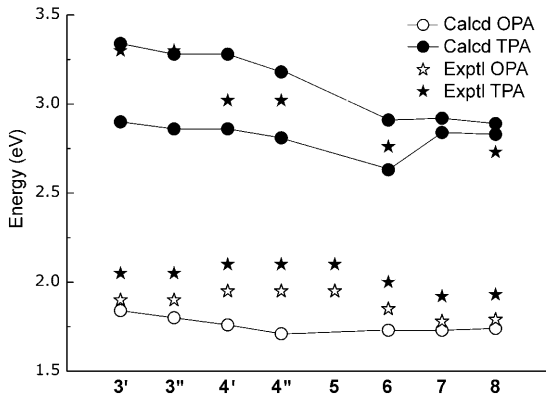

Figure 6. INDO/MRDCIS-calculated OPA and TPA state energies for compounds **3**–**8** and experimental values for **3**,[18] **4** and **6**,[13] **5**,[15] and **7** and **8** (see Supporting Information). For **3** and **4**, the theoretical data are obtained for two conformations while the same experimental data (which refer to an equilibrium mixture of conformations) are plotted twice.

tion of the HOMO and LUMO (which are the key orbitals involved in the lowest OPA and TPA transitions) in the central unit between the two indole nitrogen atoms (Figure 3). The insensitivity to extended conjugation in compounds of group III can be contrasted to that in the group IV model squaraines in which the terminal donor is in direct conjugation with the acceptor, as shown in Figure 5. The insensitivity of both peak 1 and peak 3 states to extension in group III compounds is fully reproduced in D′-D-π-C_4O_2-π-D-D′-type model structures. In a series of compounds constructed in this way, **9-1**, **11**, and **12** (see also Figures S3-1 and S3-2 of the Supporting Information for more details), the evolution of the first and second TPA active-state energies remained essentially independent of the length of π conjugation beyond the primary donor group. Thus, a π-conjugation extension of the molecules beyond the primary donor group cannot participate effectively in the conjugation with the core moiety and, thus, is not able to sufficiently stabilize the lowest TPA state to explain the origin of peak 2.

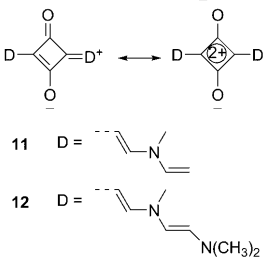

Even though indole groups block through-conjugation into the thienyl and aminostyryl substituents of the group III chromophores, the actual structure of the terminal groups nonetheless plays an important role in quantitatively determining the overall nonlinear optical properties. To get a better quantitative understanding of the δ values calculated with the correction-vector method (CVM), see Table 1, we also used the three-state model [Eq. (1)], which includes the transition dipole moments between the initial and intermediate states, μ_{01}, and between the intermediate and final states, μ_{12}, and the transition energies E_{01} and E_{02} between the relevant excited states and the ground state.

Table 1. TPA cross-section values into the 3Ag state in **4** (top) and **8** (bottom) calculated with the correction vector method (CVM), δ_{CVM}, and a three-state model, $\delta_{3\text{-state}}$, with the corresponding three-state parameters from MR-DCI calculations with singles.

	E [eV]	μ_{01} [D]	μ_{12} [D]	$\delta_{3\text{-state}}$ [GM]	δ_{CVM} [GM]
$1B_u$	1.76	13			
$3A_g$	2.86		5.6	4.0×10^5	2.8×10^3
	E [eV]	μ_{01} [D]	μ_{12} [D]	$\delta_{3\text{-state}}$ [GM]	δ_{CVM} [GM]
$1B_u$	1.74	15			
$3A_g$	2.89		7.1	1.1×10^6	7.7×10^3

$$\delta_{3\text{-state}} \sim \mu_{01}^2 \times \mu_{12}^2 \times \left(\frac{E_{02}}{E_{01}-E_{02}/2}\right)^2 \quad (1)$$

From Table 1, it can be seen that both the simple three-state model and CVM approach predict an increase in TPA cross section into the $3A_g$ state (peak 3) with conjugation length, that is, in going from **4** to **8**. From the parameters entering Equation (1), is it clear that this increase in δ upon extending the conjugated bridge is caused by an increase in the transition dipole moments μ_{01} and μ_{12} and, to a much lesser extent, by a slighly enlarged resonance enhancement factor, $E_{02}/(E_{01}-E_{02}/2)$. This calculated trend is in agreement with experiment[15] as the cross section associated with the second TPA peak (peak 3) is measured to be higher for **8** than for **5** ($\delta=4000$ and ≈750 GM,[15] respectively). It is important to note that the number of π-electrons has direct impact on the nA_g states ($n>2$), but relatively little effect on the strength of peak 2, that is, transitions to the $2A_g$ state. However, the significantly higher computational cost associated with modeling the NLO properties of complexes

with such large numbers of π-electrons makes a quantitative comparison between theory and experiment a challenging task.

The contribution of the donor group to the major molecular orbitals of the low-lying excited states determines the electronic properties of the squaraines in groups I, II and III. From our studies, we conclude that peak 2 in group **I** squaraines can be attributed to an electronically TPA-allowed state ($2A_g$) lying close in energy to the lowest energy OPA state (although the possibility of additional vibronic contributions cannot be ruled out). In contrast, the experimentally observed peak 2 in squaraines from groups II and III with indolinylidenemethyl donor fragments cannot be explained in terms of an electronic origin. We now turn to an examination of the role of vibronic coupling.

Formation of a low-lying TPA active state (peak 2) due to vibronic coupling: To obtain a physical insight into the origin of peak 2 in group II and III compounds, we have explored vibronic coupling within Herzberg–Teller (HT) theory as a possible mechanism. Note that, given the approximations related to the implementation of HT theory, it is not expected that the absolute values of the TPA cross sections computed by this means be quantitatively accurate;[33] also, the experimental cross sections cannot directly be compared in all cases to the calculated degenerate TPA cross sections, since the experimental data for peak 2 in some of the compounds are based on non-degenerate TPA measurements. Nevertheless, a qualitative description of vibrational coupling can be achieved, in particular, since our implementation of HT theory allows us to investigate the relevance of the various vibrational modes and electronic states in enabling TPA activity.

Due to the C_{2h} symmetry of squaraine **3**, only vibrational modes of b_u symmetry can mix with the OPA active $1B_u$ state to result in a TPA active $2A_g$ state. Theoretically, vibrational modes of both b_u and a_u symmetries can lead to TPA transitions: $A_g \rightarrow A_g$ and $A_g \rightarrow B_g$, respectively. However, as pointed out by Scherer et al.,[13] one can rule out the possibility that peak 2 is due to an $A_g \rightarrow B_g$ transition in centrosymmetric squaraine molecules such as **4** from an analysis of the polarization ratio (ratio of TPA cross sections in circularly and linearly polarized light) obtained with the two-photon fluorescence technique. Therefore, only b_u vibrational modes are considered here in our study of the vibronically allowed TPA process. From an examination of the adiabatic vibronic coupling constants, we found that in squaraine **3** very few (only 5 out of 48) b_u normal modes strongly couple the one-photon active $1B_u$ state with the TPA active $3A_g$ state. We note that, although additional b_u modes could, in principle, strongly couple the $1B_u$ state with higher lying nA_g states, their contributions to the two-photon cross section will be relatively small due to the larger energy differences from the $1B_u$ state. Table 2 provides the adiabatic vibronic coupling constant values between the $1B_u$ and $3A_g$ states. We identified that mode 131 (illustrated in Figure 7) gives rise to a significantly higher TPA cross section for the $1A_g \rightarrow 2A_g$ ($=1B_u \times nb_u$) transition than all the other b_u modes. Table 3 demonstrates the effect of vibronic coupling: the TPA transition $1A_g \rightarrow 2A_g$ around 2.05 eV ($\delta \approx 8$ GM) is due to mode 131. According to our calculations, the separation between $1B_u$ and $2A_g$ is 0.18 eV; this is in very good agreement with the experimental difference in state energy between peak 1 and peak 2, especially considering the approximations involved in our vibronic calculation. It is interesting to note that mode 131 is also strongly IR active.

Table 2. Strongly coupled b_u modes with their coupling strength between the $1B_u$ and 2 A_g ($=1B_u \times b_u$) state.

Mode No.	Frequency [cm^{-1}]	Adiabatic coupling [cm^{-1}]
99	1240	−566
107	1362	−681
113	1417	1161
123	1493	510
131	1590	−2098

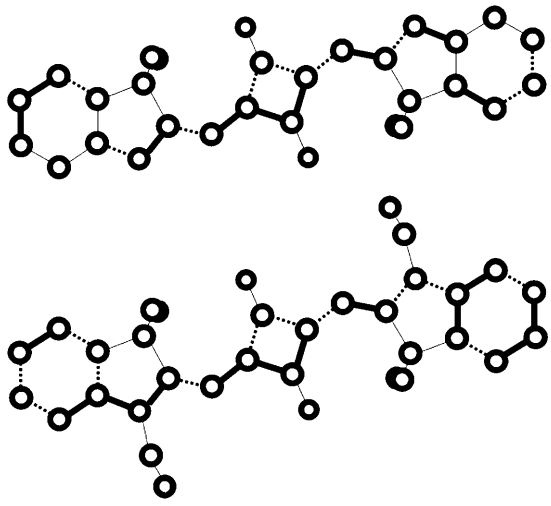

Figure 7. Schematic representation of the b_u stretching mode 131 in **3** (top) and mode 159 in **4** (bottom); elongated [compressed] bonds are shown with bold [dotted] line.

Table 3. Electronic and vibronic contributions to TPA cross section values in **3** (top) and **4** (bottom) computed at the B3LYP/SV(P)//INDO/MR-DCI singles level, using the HT vibronic coupling model.

Peak		E [eV]	$\delta^{[a]}$ [GM]	$\delta^{[b]}$ [GM]
1	$1B_u$	1.87	–	–
2	$\mathbf{2A_g = 1B_u \times b_u}$	**2.05**	**–**	**7.61**
3	$3A_g$	2.89	122	N/A
Peak		E [eV]	$\delta^{[a]}$ [GM]	$\delta^{[b]}$ [GM]
1	$1B_u$	2.08	–	–
2	$\mathbf{2A_g = 1B_u \times b_u}$	**2.27**	**–**	**33.9**
3	$3A_g$	3.16	244	N/A

[a] Without HT coupling. [b] With HT coupling.

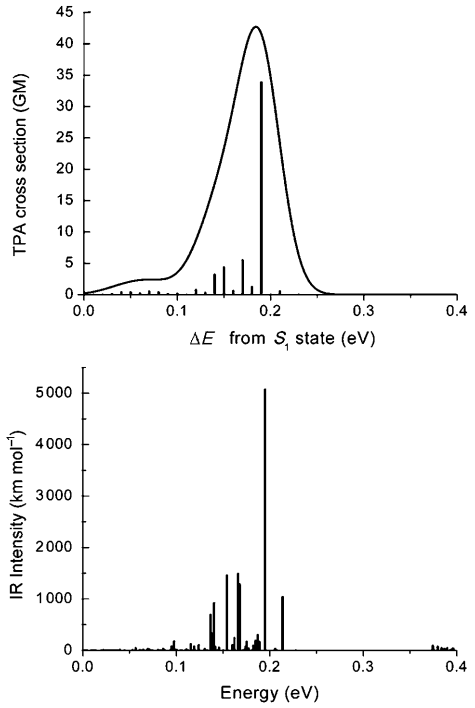

Figure 8. TPA cross-section values obtained at the B3LYP/SV(P)//INDO/MR-DCI singles level using the HT vibronic coupling model (top) and IR spectrum computed at the B3LYP/SV(P) level (bottom) for **4**. Also shown is the Gaussian convolution of the calculated TPA spectrum using a FWHM of 5 meV.

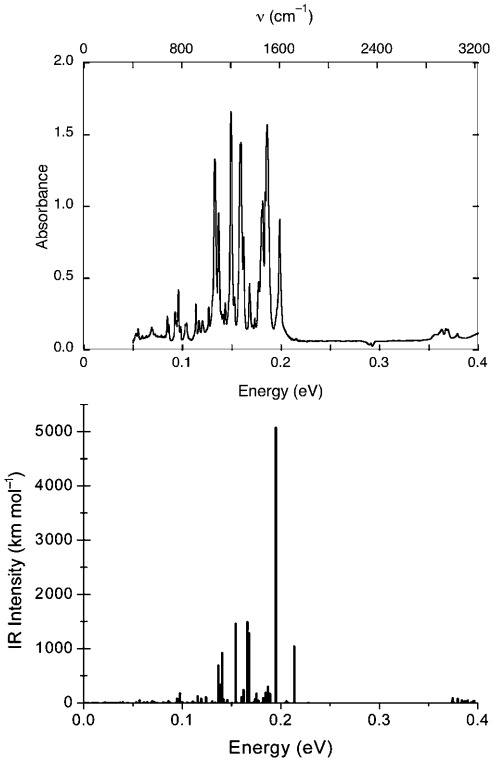

Figure 9. Experimental IR spectrum of **4** in KBr (top) and IR spectrum computed at the B3LYP/SV(P) level (bottom) for **4**.

HT vibronic coupling was also investigated in squaraine **4**. Unlike squaraine **3**, the centrosymmetric conformer of this compound (**4′**) does not have C_{2h} but C_i symmetry due to a slight twist from planarity; thus, all the normal modes were taken into account to compute the vibronic coupling. The top panel in Figure 8 shows the TPA cross-section values due to HT vibronic coupling in molecule **4**. Although strictly speaking the TPA active vibronic states do not have b_u symmetry, we can get an indication from the IR spectrum (considering the correlation between strength of IR activity and magnitude of vibronic coupling constant in squaraine **3**) of which modes could yield large TPA cross-section values through HT vibronic coupling. We observe that the effect of vibronic coupling on TPA cross section is significantly higher in mode 159 (see Figure 7) compared to other normal modes. As with squaraine **3**, inclusion of vibronic coupling in squaraine **4** leads to a predicted peak 2 that is 0.19 eV higher in state energy than peak 1; in this case, the predicted TPA cross section is somewhat larger (34 GM). Further analysis of mode 131 in squaraine **3** and mode 159 in squaraine **4** indicates that they both correspond to stretching modes impacting the degree of bond-length alternations; it is expected that the extent of bond-length alternation can affect both IR intensity and vibronic coupling strength (Figures 7 and 8).

To demonstrate that the vibrational characteristics of these molecules are computationally well-described, the experimental IR spectrum of **4** is shown in Figure 9. The computed frequencies are slightly overestimated relative to the experimental values, as is typical for the method. There is also an apparent discrepancy in the relative intensities of different modes between the experimental and theoretical spectra; in particular, in contrast to theory, the experimental peak at 0.19 eV is not the most intense peak. However, it should be noted that the 0.19 eV band is broader than all the others in the experimental spectrum, while the theory includes no broadening; when properly considering integrated oscillator strengths, the theoretical spectrum is in considerably better agreement with experiment than a cursory inspection of peak intensities might suggest. Thus, overall, the experimental and computational spectra are indeed in good agreement.

Conclusion

We have shown that the origin of peak 2 in squaraines is dependent on the nature of substituent donor moiety, changing from predominantly electronic (e.g., in diarylaminothienyl donors) to vibronic (e.g., in indolinylidenemethyl donors) in character. For squaraines with diarylaminothienyl donors (group I), the lowest TPA active electronic state ($2A_g$, peak 2) is located close in energy to the $1B_u$ (peak 1) state, thus providing a purely electronic channel for TPA into peak 2 (although one cannot rule out additional contributions from vibronic coupling), which corresponds to the sce-

nario on the middle in Figure 1. On the other hand, the lowest electronic TPA active state ($3A_g$) is energetically well-separated from the $1B_u$ state for all squaraines containing indolinylidenemethyl donors (groups II and III), which corresponds to scenario on the right in Figure 1.

The possibility of a vibronic origin for peak 2 in group II and III molecules was investigated by using an efficient implementation of HT theory in conjunction with the ZINDO Hamiltonian. These calculations confirmed the previous suggestion of Scherer and co-workers[13] of a vibronic origin for peak 2 in this class of chromophores. The experimental TPA absorption peak 2 in compounds of groups II and III is rather sharp, which suggests that only a few modes are strongly coupled with the $1B_u$ state and dominate contributions to the TPA cross section. Our calculations confirm that this is indeed the case for squaraine molecules containing indolinylidenemethyl fragments and provide an explanation for the energy and lineshape of the experimentally observed peak 2 in these compounds.

Computational Details

All calculations were performed without consideration of solvent effects, since centrosymmetric squaraines show only very slight solvatochromism in both absorption and fluorescence spectra.[22] All squaraine geometries were optimized at the DFT/B3LYP[34] level of theory using the SV(P)[35] basis set, (equivalent to 6-31G* basis set) as implemented in the TURBOMOLE package.[36–38]

Based on DFT-optimized geometries, the excited-state energies and state- and transition-dipole moments were evaluated with the semiempirical intermediate neglect of differential overlap (INDO) Hamiltonian[39,40] coupled to a multireference determinant single and double configuration interaction (MRD-CI[41] with singles (S) or singles and doubles (SD)) scheme by using the Mataga–Nishimoto potential to express the Coulomb repulsion term.[42,43] As we use large CI active spaces for computational accuracy, MRD-CISD is computationally expensive for large systems. Hence, this method was only used for the smaller squaraines. MRD-CIS was used to determine state energies of the squaraines **1**–**12**. In all the MRD-CIS and MRD-CISD calculations, Rumer CI diagrams were generated from the reference closed-shell Hartree–Fock (HF) ground-state determinant and four excited determinants: HOMO−1→LUMO, HOMO→LUMO, HOMO→LUMO+1, and (HOMO, HOMO)→(LUMO, LUMO). The TPA cross-section values were computed with either the perturbative sum-over-states (SOS) method of Orr and Ward[44] (including the 300 lowest-lying states) or the correction vector method (CVM).[45] The truncation to 300 states in the SOS method can, in some cases, introduce an uncontrolled error.[45] Since this problem is avoided in CVM, we use this approach to check the validity of the SOS TPA cross-section values. While with the SOS method one can take into account only a finite number of excited states due to the large memory requirement of the calculations, in CVM, the TPA calculation requires only the lowest eigenvalue and eigenvector. Therefore, a larger number of configurations compared with the SOS method can be handled. We implemented Davidson's diagonalization algorithm[46] to obtain the low-lying eigenvalues and eigenvectors of large CI matrices which were then used in CVM for TPA cross-section calculations. The size of the CI active space was increased until the first excited states converged to their experimental values.

As it is essential in our study to obtain very accurate energies of low-lying excited states, we used the ab initio size-consistent CIS(D)[47,48] (as implemented in Q-Chem 3.0[49]), TD-DFT,[50–52] INDO/CCSD[53] (coupled cluster singles and doubles) and INDO/CIS methods besides INDO/MRDCI approach to investigate the nature of the low-lying energy levels. Based on comparison of different methods we concluded that the INDO/MRDCI method with single excitations (MRD-CIS) is both reliable and computationally feasible for handling large CI active space required for the squaraines in our study. Details of the electronic and optical properties computed from all the methods discussed here are available in the Supporting Information.

Although using an ab initio TD-DFT based approach to compute the TPA cross section in quadrupolar molecules like squaraines could be an attractive alternative to an INDO/MRDCI-based approach, we are unaware of any successful attempt in the literature of such applications to calculating the TPA of quadrupolar molecules. We note that the nonlinear polarizabilities in TD-DFT-based approaches are often overestimated, which can be attributed to the lack of orbital-dependent terms in the exchange correlation potential or self-interaction error.[54] Lately, there have been some successes in the evaluation of the NLO properties of dipolar molecules by using long-range correction schemes in the exchange-correlation functional; however, further improvements would be required to correctly reflect the multiple excitation character of the higher lying excited states before such approaches can be applied to quadrupolar systems. Further details of the quantum-chemical calculations are available in the Supporting Information.

Following an analysis of the vibrational frequencies obtained from DFT calculations at the B3LYP/SV(P) level, the adiabatic vibronic coupling constants were computed from a 25×25 Rumer basis MRD-CIS calculation using the ground-state HF determinant and two excited configurations (HOMO→LUMO, HOMO→LUMO+1) as references. We incorporated the vibronic effect within the HT theory using the floating atomic orbital (FAO) approach[55] in ZINDO. The FAO approach is known to give much better convergence than the direct implementation of HT expansion. The sparse matrix approach was implemented to ensure efficiency. Details of the implementation in ZINDO and subsequent applications will be published elsewhere.[56]

In general, either the ground or intermediate or final electronic state could couple with vibrational modes to contribute to the TPA cross section. However, the only term relevant for the problem in hand is the perturbation of the final state ($1B_u$), for which the vibronically allowed part of the tensor can be written as Equation (2):

$$S^{g0,fv}_{\alpha,\beta} = \langle \chi^g_0 | Q | \chi^f_v \rangle \sum_{ij} \frac{V_{fj}(\mu_{\alpha,gi}\mu_{\beta,ij} + \mu_{\alpha,ij}\mu_{\beta,gi})}{E^0_i - E^0_g - \hbar\omega}$$
$$V_{ij} = \left\langle \frac{\bar{\Psi}^0_i(\mathrm{Q})|(\partial H/\partial Q_0)|\bar{\Psi}^0_j(Q)}{\bar{E}^0_j - \bar{E}^0_i} \right\rangle \qquad (2)$$

in which the vibrational integral ($\langle \chi^g_0 | Q | \chi^f_v \rangle$)is calculated (in zeroth-order approximation)[57] between the 0th vibrational wavefunction of the ground state and vth vibrational wavefunction of the final state; $\mu_{\alpha,ij}$ and $\mu_{\beta,ij}$ are x, y, z components of the transition dipole moment between states i and j, and V_{ij} is the vibronic coupling between states i and j ($\bar{\Psi}$ and $\bar{E}$ denote the wavefunction and energy in the FAO basis). The TPA cross section, δ, due to vibronic coupling was computed using the S-tensor approach[58,59] for squaraines **3** and **4**.

Acknowledgements

We are most grateful to Eric Van Stryland, David Hagan, Lazaro Padilha, and Jie Fu from the University of Central Florida for graciously providing us with the experimental spectra for compounds **2**, **7**, and **8**. We thank DARPA for support through the MORPH program (Grant ONR N00014-04-0095). The work at Georgia Tech has also been supported in part by the National Science Foundation through the Science and Technology Center Program, under Award DMR-0120967, and the CRIF Program, under Award CHE-0443564.

[1] M. Albota, D. Beljonne, J.-L. Brédas, J. E. Ehrlich, J.-Y. Fu, A. A. Heikal, S. E. Hess, T. Kogej, M. D. Levin, S. R. Marder, D. McCord-Maughon, J. W. Perry, H. Röckel, M. Rumi, G. Subramaniam, W. W. Webb, X.-L. Wu, C. Xu, *Science* **1998**, *281*, 1653.
[2] S. J. Chung, M. Rumi, V. Alain, S. Barlow, J. W. Perry, S. R. Marder, *J. Am. Chem. Soc.* **2005**, *127*, 10844.
[3] T.-C. Lin, S.-J. Chung, K.-S. Kim, X. Wang, G. S. He, J. Swiatkiewicz, H. E. Pudavar, P. N. Prasad, *Adv. Polym. Sci.* **2003**, *161*, 157.
[4] S. J. K. Pond, M. Rumi, M. D. Levin, T. C. Parker, D. Beljonne, M. W. Day, J. L. Bredas, S. R. Marder, J. W. Perry, *J. Phys. Chem. A* **2002**, *106*, 11470.
[5] B. Strehmel, A. M. Sarker, H. Detert, *ChemPhysChem* **2003**, *4*, 249.
[6] S. R. Marder, J. L. Brédas, J. W. Perry, *MRS Bull.* **2007**, *32*, 561.
[7] J. H. Andrews, K. D. Singer, C. W. Dirk, D. L. Hull, K. C. Chuang, *Proc. SPIE-Int. Soc. Opt. Eng.* **1998**, *3473*, 68.
[8] R. W. Bigelow, H.-J. Freund, *Chem. Phys.* **1986**, *107*, 159.
[9] C.-T. Chen, S. R. Marder, L.-T. Cheng, *J. Am. Chem. Soc.* **1994**, *116*, 3117.
[10] C. W. Dirk, L. T. Cheng, M. G. Kuzyk, *Int. J. Quant. Chem.* **1992**, *43*, 27.
[11] K. S. Mathis, M. G. Kuzyk, C. W. Dirk, A. Tan, S. Martinez, G. Gampos, *J. Opt. Soc. Am. B* **1998**, *15*, 871.
[12] F. Meyers, C. T. Chen, S. R. Marder, J. L. Bredas, *Chem. Eur. J.* **1997**, *3*, 530.
[13] D. Scherer, R. Dorfler, A. Feldner, T. Vogtmann, M. Schwoerer, U. Lawrentz, W. Grahn, C. Lambert, *Chem. Phys.* **2002**, *279*, 179.
[14] Q. L. Zhou, R. F. Shi, O. Zamani-Khamari, A. F. Garito, *Mol. Cryst. Liq. Cryst. Sci. Technol. Sect. B* **1993**, *145*, 6.
[15] J. Fu, L. A. Padilha, D. J. Hagan, E. W. Van Stryland, O. V. Przhonska, M. V. Bondar, Y. L. Slominsky, A. D. Kachkovski, *J. Opt. Soc. Am. B* **2007**, *24*, 67.
[16] S. J. Chung, S. J. Zheng, T. Odani, L. Beverina, J. Fu, L. A. Padilha, A. Biesso, J. M. Hales, X. W. Zhan, K. Schmidt, A. J. Ye, E. Zojer, S. Barlow, D. J. Hagan, E. W. Van Stryland, Y. P. Yi, Z. G. Shuai, G. A. Pagani, J. L. Bredas, J. W. Perry, S. R. Marder, *J. Am. Chem. Soc.* **2006**, *128*, 14444.
[17] J. Andrews, J. Khaydarov, K. Singer, *Opt. Lett.* **1994**, *19*, 984.
[18] J. Andrews, J. Khaydarov, K. Singer, D. Hull, K. Chuang, *J. Opt. Soc. Am. B* **1995**, *12*, 2360.
[19] Y. Yu, R. Shi, A. Garito, C. Grossman, *Opt. Lett.* **1994**, *19*, 786.
[20] C. Poga, T. Brown, M. Kuzyk, C. Dirk, *J. Opt. Soc. Am. B* **1995**, *12*, 531.
[21] C. W. Dirk, W. C. Herndon, F. Cervanteslee, H. Selnau, S. Martinez, P. Kalamegham, A. Tan, G. Campos, M. Velez, J. Zyss, I. Ledoux, L. T. Cheng, *J. Am. Chem. Soc.* **1995**, *117*, 2214.
[22] F. Terenziani, A. Painelli, C. Katan, M. Charlot, M. Blanchard-Desce, *J. Am. Chem. Soc.* **2006**, *128*, 15742.
[23] P. M. Kazmaier, G. K. Hamer, R. A. Burt, *Can. J. Chem.* **1990**, *68*, 530.
[24] G. Herzberg, E. Teller, *Z. Phys. Chem. Abt. B* **1933**, *21*, 410.
[25] M. Sheik-bahae, A. A. Said, E. W. Van Stryland, *Opt. Lett.* **1989**, *14*, 955.
[26] M. Sheik-bahae, A. A. Said, T.-H. Wei, D. J. Hagan, E. W. Van Stryland, *IEEE J. Quantum Electron.* **1999**, *26*, 760.
[27] R. A. Negres, J. M. Hales, A. Kobyakov, D. J. Hagan, E. W. Van Stryland, *Opt. Lett.* **2002**, *27*, 270.
[28] J. M. Hales, D. J. Hagan, E. W. Van Stryland, K. J. Schafer, A. R. Morales, K. D. Belfield, P. Pacher, O. Kwon, E. Zojer, J. L. Bredas, *J. Chem. Phys.* . **2004**, 121.
[29] Y. Kobayashi, M. Goto, M. Kurahashi, *Bull. Chem. Soc. Jpn.* **1986**, *59*, 311.
[30] J. R. Heflin, A. F. Garito, in *Electroresponsive Molecular and Polymeric Systems, Vol. 2* (Ed.: T. A. Skotheim), Marcel Dekker, New York, **1991**, p. 113.
[31] M. G. Kuzyk, C. W. Dirk, *Phys. Rev. A* **1990**, *41*, 5098.
[32] B. M. Pierce, *J. Chem. Phys.* **1989**, *91*, 791.
[33] G. Marconi, G. Orlandi, *J. Chem. Soc. Faraday Trans. 2* **1982**, *78*, 565.
[34] A. D. Becke, *J. Chem. Phys.* **1993**, *98*, 5648.
[35] A. Schäfer, H. Horn, R. Ahlrichs, *J. Chem. Phys.* **1992**, *97*, 2571.
[36] R. Bauernschmitt, R. Ahlrichs, *Chem. Phys. Lett.* **1996**, *256*, 454.
[37] F. Furche, R. Ahlrichs, *J. Chem. Phys.* **2002**, *117*, 7433.
[38] For current version see: http://www.turbomole.de.
[39] A. Pople, D. L. Beveridge, P. A. Dobosh, *J. Chem. Phys.* **1967**, *47*, 2026.
[40] J. Ridley, M. Zerner, *Theor. Chim. Acta.* **1973**, *32*, 111.
[41] D. Beljonne, G. O'Keefe, P. Hamer, R. Friend, H. Anderson, J. Brédas, *J. Chem. Phys.* **1997**, *106*, 9439.
[42] N. Mataga, K. Nishimoto, *Z. Phys. Chem.* **1957**, *13*, 140.
[43] M. C. Zerner, G. H. Loew, R. F. Kichner, U. T. Mueller-Westerhoff, *J. Am. Chem. Soc.* **1980**, *102*, 589.
[44] B. Orr, J. Ward, *Mol. Phys.* **1971**, *20*, 513.
[45] S. Ramasesha, Z. Shuai, J. Bredas, *Chem. Phys. Lett.* **1995**, *245*, 224.
[46] S. R. Langhoff, E. R. Davidson, *Int. J. Quantum Chem.* **1974**, *8*, 61.
[47] N. Besley, M. Oakley, A. Cowan, J. Hirst, *J. Am. Chem. Soc.* **2004**, *126*, 13502.
[48] N. Besley, *J. Chem. Phys.* **2005**, *122*, 184706.
[49] Y. Shao L. F.-M. , Y. Jung, J. Kussmann, C. Ochsenfeld, S. T. Brown, A. T. B. Gilbert, L. V. Slipchenko, S. V. Levchenko, D. P. O'Neill, R. A. Distasio Jr. , R. C. Lochan, T. Wang, G. J. O. Beran, N. A. Besley, J. M. Herbert, C. Y. Lin, T. Van Voorhis, S. H. Chien, A. Sodt, R. P. Steele, V. A. Rassolov, P. E. Maslen, P. P. Korambath, R. D. Adamson, B. Austin, J. Baker, E. F. C. Byrd, H. Dachsel, R. J. Doerksen, A. Dreuw, B. D. Dunietz, A. D. Dutoi, T. R. Furlani, S. R. Gwaltney, A. Heyden, S. Hirata, C.-P. Hsu, G. Kedziora, R. Z. Khalliulin, P. Klunzinger, A. M. Lee, M. S. Lee, W. Liang, I. Lotan, N. Nair, B. Peters, E. I. Proynov, P. A. Pieniazek, Y. M. Rhee, J. Ritchie, E. Rosta, C. D. Sherrill, A. C. Simmonett, J. E. Subotnik, H. L. Woodcock III, W. Zhang, A. T. Bell, A. K. Chakraborty, D. M. Chipman, F. J. Keil, A. Warshel, W. J. Hehre, H. F. Schaefer III, J. Kong, A. I. Krylov, P. M. W. Gill, M. Head-Gordon, *Phys. Chem. Chem. Phys.* **2006**, *8*, 3172
[50] E. Runge, E. Gross, *Phys. Rev. Lett.* **1984**, *52*, 997.
[51] E. Gross, *Adv. Quantum Chem.* **1990**, *21*, 255.
[52] E. Gross, J. Dobson, M. Petersilka, *Top. Curr. Chem.* **1996**.
[53] R. Buenker, S. Peyerimhoff, *Theor. Chim. Acta.* **1974**, *35*, 33.
[54] M. Kamiya, H. Sekino, T. Tsuneda, K. Hirao, *J. Chem. Phys.* **2005**, *122*, 10.
[55] G. Orlandi, *Chem. Phys. Lett.* **1976**, *44*, 277.
[56] I. Rudra, S. Ohira, K. Schmidt, J. L. Bredas, unpublished results.
[57] P. Macak, Y. Luo, H. Agren, *Chem. Phys. Lett.* **2000**, *330*, 447.
[58] P. Monson, W. McClain, *J. Chem. Phys.* **1970**, *53*, 29.
[59] W. Peticolas, *Annu. Rev. Phys. Chem.* **1967**, *18*, 233.

Received: May 30, 2008
Published online: October 29, 2008

